

See discussions, stats, and author profiles for this publication at: <https://www.researchgate.net/publication/328991226>

# A New Registration Algorithm for Multimodal Remote Sensing Images

Conference Paper · July 2018

DOI: 10.1109/IGARSS.2018.8517853

---

CITATIONS

7

---

READS

177

4 authors, including:



Xie xw

Wuhan University

9 PUBLICATIONS 95 CITATIONS

SEE PROFILE



Xiao Ling

The Ohio State University

28 PUBLICATIONS 288 CITATIONS

SEE PROFILE



Wang Xiang

Wuhan University

8 PUBLICATIONS 94 CITATIONS

SEE PROFILE

# A NEW REGISTRATION ALGORITHM FOR MULTIMODAL REMOTE SENSING IMAGES

*Xunwei Xie, Yongjun Zhang\*, Xiao Ling, Xiang Wang*

School of Remote Sensing and Information Engineering, Wuhan University, P.R. China

## ABSTRACT

Automatic registration of remote sensing images is a challenging problem in the applications of remote sensing. The multimodal remote sensing images have significant nonlinear radiometric differences, which lead to the failure of area-based and feature-based registration methods. In this paper, to overcome significant nonlinear radiometric differences and large scale differences of multimodal remote sensing images, we propose a new registration algorithm, which can meet the need of initial registration of multimodal remote sensing images that conform to similarity transformation model. Our synthetic and real-data experimental results demonstrate the effectiveness and good performance of the proposed method in terms of visualization and registration accuracy.

*Index Terms*— Multimodal remote sensing images, Log-Gabor filter, multi-scale atlas, phase correlation, image registration

## 1. INTRODUCTION

Image registration is a fundamental and crucial problem in remote sensing analysis tasks including change detection, image fusion, and image mosaic [1-3]. And it is to essentially overlap two or more images, and align the reference image and sensed image [1].

During the last decades, there have been rapid developments of image registration methods, which are mainly divided into area-based methods and feature-based methods. However, these methods cannot satisfy the need of multimodal remote sensing image registration because of significant nonlinear radiometric differences and the remarkable geometric differences. The common way to deal with geometric differences is to apply the imaging physical model to eliminate the global rotation and scale differences [4]. However, the remained local geometric differences should be taken into account to improve the robustness of registration methods.

To address the above issues, we extend traditional phase correlation method [5, 6] based on multi-scale Log-Gabor [7] filtering, which can effectively solve the situation caused by significant nonlinear radiometric differences and large scale

differences. And we call our method as MLPC for convenience. The remainder of this paper is organized as follows. Section 2 describes related work. Section 3 presents some details of MLPC. Section 4 illustrates the rationality of MLPC on synthetic images, and the registration performance of MLPC on a multimodal image pair. In final, conclusion is arranged in section 5.

## 2. RELATED WORK

Generally, image registration consists of four steps: feature detection, feature matching, transformation model estimation and image resampling and transformation [1]. There are two main approaches to feature understanding: area-based and feature-based. The former puts emphasis on the feature matching rather than detection, whereas the latter seeks the correspondences with similar descriptors between local features.

In area-based registration methods, Normalized Cross Correlation (NCC) is a classical representative [8], whose idea is to compute the similarity metrics of the two windows and consider the most similar one as a correspondence. However, the area-based methods are not robust to the situation where the regions lack texture. The Fourier methods are also used to image registration [9], which are efficient and robust to the dependent noises in frequency domain. The mutual information (MI) methods work directly with image intensities, which are not insensitive to local differences, so they are suitable for multimodal image registration [10]. However, its shortcoming is the big budget. Feature-based methods first extract the features of interest, and find the correspondences with similar local descriptors. The most widely used feature descriptors in remote sensing are SIFT [11]. However, when they are applied to process multimodal images, the significant nonlinear radiometric differences will cause the contrast change between various features, making it difficult to extract highly repeatable shared features and describe their feature vectors, further degrading the performance of registration methods [12].

As the geometric structural information of the same features may be kept the same in the multimodal remote sensing images, thus the images can be registered through the consistency of geometric structural information. The Log-Gabor filter is an effective means to obtain the

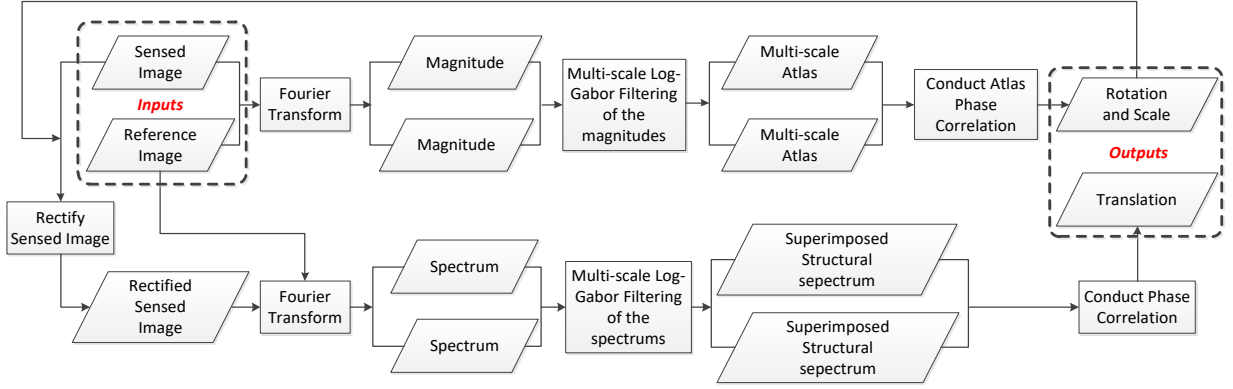


Fig. 1. Flowchart of the proposed method (MLPC).

geometric structural information [7], which is insensitive to local radiometric differences and independent of image luminance, compared with contour gradient based methods. Therefore, it is usually utilized to assist image registration.

Phase correlation algorithm, proposed by Kuglin [13], and developed by Foroosh [14] and Reddy [6], is used to register two images that conform to the similarity transformation model. Combining phase correlation and other descriptors, a good initial registration result can be obtained. However, it cannot handle significant radiometric differences and large scale differences between images.

### 3. PROPOSED METHOD

We choose the similarity transformation model (i.e. rotation, scale, and translation) to express the global relationship between the reference and sensed images. The proposed method (MLPC) is divided into two parts as the entire flowchart shown in Fig.1. As some steps of MLPC are identical with the traditional extended phase correlation algorithm, we then only put emphasis on the special keys.

#### 3.1. Multi-scale Log-Gabor filtering of the magnitudes

The structural information provided by Log-Gabor filter can keep highly consistent between the images with significant nonlinear radiometric differences. Inspired by this, we can obtain the magnitudes of the reference and sensed images in frequency domain after Fourier transform. And then, the magnitudes are filtered by using different kinds of Log-Gabor filters with different central frequencies, and a series of filtered images can be obtained. It is noting that the filtered images basically have no overlapping information, so we do not directly conduct phase correlation of the filtered images which have different scales. After the filtering process, we build a multi-scale atlas space in which the upper structural information will be contained in the next layer, so as to facilitate phase correlation of the filtered images. We choose three different scales in Log-Gabor filtering to build the multi-scale atlas, and the scale ratio

between adjacent scales is 2.1. The multi-scale atlas space built in this paper has the following form:

$$\begin{cases} A_1 = FI_1 \\ A_2 = \sqrt{FI_1^2 + FI_2^2} \\ A_3 = \sqrt{FI_1^2 + FI_2^2 + FI_3^2} \end{cases} \quad (1)$$

where  $FI_i$  represents the  $i^{\text{th}}$  filtered image of magnitude using Log-Gabor filter with different central frequencies;  $A_i$  represents the  $i^{\text{th}}$  layer of the multi-scale atlas space.

#### 3.2. Conduct atlas phase correlation

This step is to conduct phase correlation between every image pair in the atlases of the reference image and sensed image. We record all the peaks of all the phase correlation results, while the maximum response peak among them is considered the optimal solution. The coordinates of the maximum response peak will be utilized to calculate the scale and rotation, making use of the method proposed in [6]. And the parameters of phase correlation module also are used as the recommendation of reference [6]. Hereto, the rotation and scale differences between the reference image and sensed image are eliminated.

#### 3.3. Rectify sensed image

The sensed image is rectified via bilinear interpolation according to the rotation angle and scale factor obtained in the previous steps, and the rectified sensed image is used as new input to eliminate the translation differences to the reference image. In the real scene, we should decide whether to downscale the large scale image or upscale the small scale image according to the specific scale.

#### 3.4. Multi-scale Log-Gabor Filtering of the structural spectrums

This step is to extract the structural spectrums as far as possible, in order to eliminate the interface of radiometric differences. The structural spectrums with different scales are superimposed together. After that, the cross power spectrum between the superimposed structural spectrums of the reference image and rectified sensed image is calculated. And then, inverse Fourier Transform is conducted and the maximum peak is obtained, and the coordinates of the maximum peak will determine the translation.

#### 4. EXPERIMENTS AND ANALYSIS

The experiments are divided into two classes: synthetic experiment, which is used to evaluate the rationality of MLPC, and real-data experiment, which is used to evaluate the effectiveness of MLPC.

##### 4.1. Synthetic experiment

The reference image is shown in Fig.2 (a), with  $512 \times 512$  in size. The sensed image (Fig.2 (b)) is obtained by regional automatic balance processing of the reference image, and then rotating 30 degrees and downscaling by 4 times.

The atlas phase correlation results of the reference and sensed images are shown in Fig. 3, and only the succeeded ones that are able to successfully calculate the rotation angle and scale factor are shown. The rotation-scale pairs are  $(29.26^\circ, 3.80)$ ,  $(30.16^\circ, 3.93)$  and  $(30.42^\circ, 4.02)$  corresponding to Figs. 3(a)-3(c), respectively. The transformation model parameters calculated in Fig. 3(b) are closest to the real values, because the corresponding image pair has the same scale and highly similar structural information. We also omit the visualization results of six failed cases. In this experiment, phase correlation failure occurs when there is a big difference in the structural information between the two images, because the maximum response peak in the phase correlation module is difficult to be assured under that situation where the scale ratio between the two images is larger than 1.8 [6]. The failed cases demonstrate that it may be difficult to get the correct results by directly extracting the structural information at the original scale level. This experiment also indirectly demonstrates that it is necessary to build a multi-scale atlas space to enhance the stability of phase correlation.

##### 4.2. Real-data experiment

The two images are visible spectral and infrared images, both  $400 \times 400$  in size, as shown in Fig. 4. The overlapped area covers buildings, and the nonlinear radiometric differences between them are ubiquitous, while the structural information is almost the same.

Fig. 5 shows the registration results of MLPC. The staggered grids are utilized for the visualization of the registration details. It can be seen that MLPC can resist the

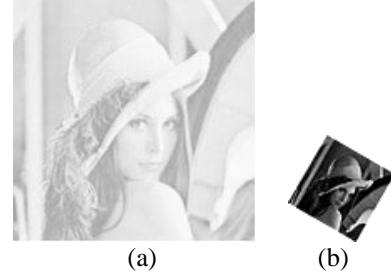


Fig. 2. Synthetic data. (a) Reference image (b) Sensed image.

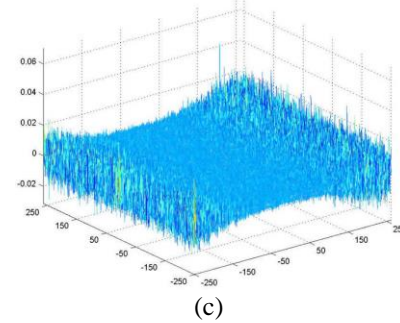
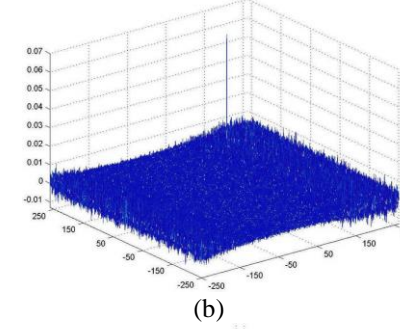
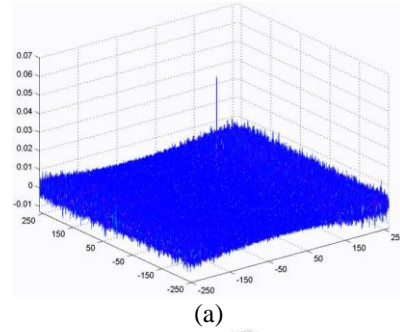


Fig. 3. Atlas phase correlation results. (a) Phase correlation result between  $A_1$  of reference image and  $A_2$  of sensed image. (b) Phase correlation result between  $A_1$  of reference image and  $A_3$  of sensed image. (c) Phase correlation result between  $A_2$  of reference image and  $A_3$  of sensed image. The location of the peak determines the rotation and scale [6].

nonlinear radiometric differences between the two images. In terms of the local registration details, MLPC qualitatively

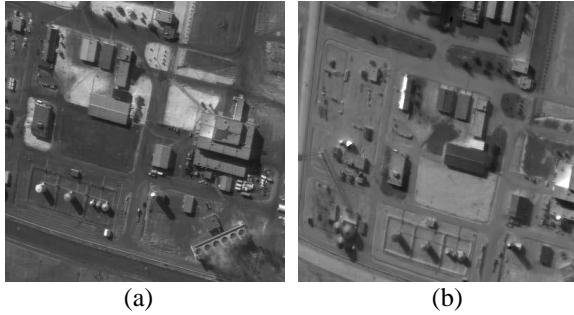


Fig. 4. Real data. (a) Reference image. (b) Sensed image.

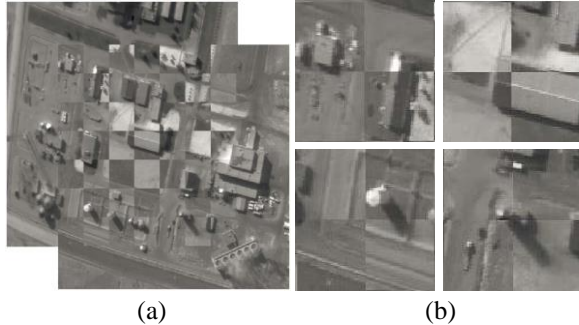


Fig. 5. Registration results. (a) Visualization result shown with staggered grids. (b) The displayed details of four different localities.

owns good registration performance. We also compared MLPC to the classical area-based method: NCC, in terms of registration accuracy. In this comparison, 30 check points were manually chosen and their residuals were counted. As the results shown in Table 1, the registration accuracy of MLPC was superior to that of NCC. The reason is that NCC cannot deal with nonlinear radiometric differences well, which affects the distribution and the quality of the correspondences and then affects the transformation model estimation. In addition, as the greedy search strategy of NCC, the transformation model estimated by MLPC was utilized as a prior of NCC to constraint NCC's search area. This indicates that our method can serve as a pretreatment of other methods.

Table 1. Registration accuracy of NCC and MLPC.

methods	RMSE (pix.)	Max error (pix.)
NCC	1.20	2.12
MLPC	0.28	1.00

## 5. CONCLUSION

In this paper, we propose a new registration method for multimodal remote sensing images, focusing on the issues caused by significant nonlinear radiometric differences and large scale differences. The synthetic and real-data experimental results help to confirm the rationality and effectiveness of the proposed method. The simple quantitative analysis result of the real-data experiment

verifies its good registration accuracy. In future work, we will further research the best multi-scale atlas building scheme used in this paper, and more quantitative comparisons with other most advanced methods using more multimodal data sets should be taken into consideration.

## ACKNOWLEDGMENTS

This research was partially supported by the National Key R&D Program of China, Grant No. 2017YFB0503004.

## REFERENCES

- [1] B. Zitova and J. Flusser, "Image registration methods: a survey," *Image and vision computing*, vol. 21, no. 4, pp. 977-1000, 2003.
- [2] R. Szeliski, *Computer vision: algorithms and applications*, Springer Science & Business Media, 2010.
- [3] A. Wong and D. A. Clausi, "ARRSI: Automatic registration of remote sensing images," *IEEE Trans. Geosci. Remote Sens.* vol. 45, no. 5, pp. 1483-1493, 2007.
- [4] Y. Duan, X. Huang, J. Xiong, Y. Zhang, and B. Wang, "A combined image matching method for chinese optical satellite imagery," *International Journal of Digital Earth*, vol. 9, no. 9, pp. 851-872, 2016.
- [5] E. De Castro and C. Morandi, "Registration of translated and rotated images using finite fourier transforms," *IEEE Trans. Pattern Anal. Mach. Intell.*, no. 5, pp. 700-703, 1987.
- [6] B. S. Reddy and B. N. Chatterji, "An fft-based technique for translation, rotation, and scale-invariant image registration," *IEEE transactions on image processing*, vol. 5, no. 8, pp. 1266-1271, 1996.
- [7] D. J. Field, "Relations between the statistics of natural images and the response properties of cortical cells," *J. Optical Soc. Amer. A.*, vol. 4, no. 12, pp. 2379-2394, 1987.
- [8] R. C. Gonzalez and P. Wintz, *Digital Image Processing*, NewYork, NY, USA: Addison-Wesley, 1987.
- [9] Q. S. Chen, M. Defrise, and F. Deconinck, "Symmetric phase-only matched filtering of Fourier-Mellin transforms for image registration and recognition," *IEEE Trans. Pattern Anal. Mach. Intell.*, vol. 16, no. 12, pp. 1156-1168, Dec. 1994.
- [10] J. Inglada, V. Muron, D. Pichard, and T. Feuvrier, "Analysis of artifacts in subpixel remote sensing image registration," *IEEE Trans. Geosci. Remote Sens.*, vol. 45, no. 1, pp. 254-264, Jan. 2007.
- [11] D. G. Lowe, "Distinctive image features from scale-invariant keypoints," *International Journal of Computer Vision*, vol. 60, no. 2, pp. 91-110, 2004.
- [12] Y. Ye and L. Shen, "Hopc: A novel similarity metric based on geometric structural properties for multi-modal remote sensing image matching," *ISPRS Annals of Photogrammetry, Remote Sensing and Spatial Information Sciences*, vol. III-1, pp. 9-16, 2016.
- [13] C. D. Kuglin and D. C. Hines, "The phase correlation image alignment method," In *Proceeding of IEEE International Conference on Cybernetics and Society*, pages 163-165, New York, USA, Sept. 1975.
- [14] H. Foroosh, J. B. Zerubia, and M. Berthod, "Extension of phase correlation to subpixel registration," *IEEE Transactions on Image Processing*, vol. 11, no. 3, pp. 188-200, Mar 2002.